

A Crossed Beam and *ab Initio* Investigation on the Formation of Boronyldiacetylene ($\text{HCCCC}^{11}\text{BO}$; $X^1\Sigma^+$) via the Reaction of the Boron Monoxide Radical (^{11}BO ; $X^2\Sigma^+$) with Diacetylene (C_4H_2 ; $X^1\Sigma_g^+$)

Dorian S. N. Parker, Nadia Balucani,[†] Domenico Stranges,[‡] and Ralf I. Kaiser*

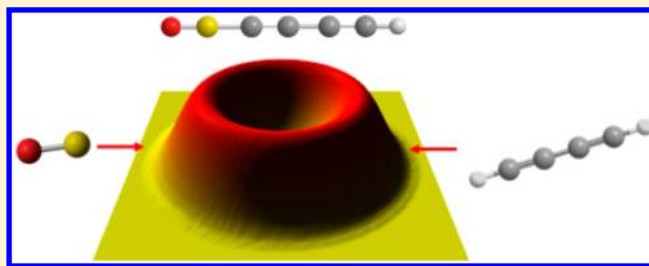
Department of Chemistry, University of Hawaii at Manoa, Honolulu, Hawaii 96822, United States

Alexander Mebel*

Department of Chemistry and Biochemistry, Florida International University, Miami, United States

S Supporting Information

ABSTRACT: The reaction dynamics of the boron monoxide radical (^{11}BO ; $X^2\Sigma^+$) with diacetylene (C_4H_2 ; $X^1\Sigma_g^+$) were investigated at a nominal collision energy of 17.5 kJ mol^{-1} employing the crossed molecular beam technique and supported by *ab initio* and statistical (RRKM) calculations. The reaction is governed by indirect (complex forming) scattering dynamics with the boron monoxide radical adding with its boron atom to the carbon–carbon triple bond of the diacetylene molecule at one of the terminal carbon atoms without entrance barrier. This leads to a doublet radical intermediate ($\text{C}_4\text{H}_2^{11}\text{BO}$), which undergoes unimolecular decomposition through hydrogen atom emission from the C1 carbon atom via a tight exit transition state located about 18 kJ mol^{-1} above the separated products. This process forms the hitherto elusive boronyldiacetylene molecule ($\text{HCCCC}^{11}\text{BO}$; $X^1\Sigma^+$) in a bimolecular gas phase reaction under single collision conditions. The overall reaction was determined to be exoergic by 62 kJ mol^{-1} . The reaction dynamics are compared to the isoelectronic diacetylene (C_4H_2 ; $X^1\Sigma_g^+$)–cyano radical (CN ; $X^2\Sigma^+$) system studied previously in our group. The characteristics of boronyldiacetylene and the boronyldiacetylene molecule ($\text{HCCCC}^{11}\text{BO}$; $X^1\Sigma^+$) as well as numerous intermediates are reported for the first time.



1. INTRODUCTION

The energy release from hydrocarbon oxidation powers the mainstream of internal combustion engines. Boron combustion has been probed to provide almost three times the energy by weight and volume compared to hydrocarbons—attributes that are attractive to rocket propulsion systems in space exploration and for military purposes.^{1–3} Unfortunately, in the initial stages of combustion, solid state boron forms a highly inert layer of diboron trioxide (B_2O_3) which prevents oxidation and effective energy release of the boron material.^{4–7} Currently, boron is used as pellet additives in conventional hydrocarbon-based rocket fuels.⁴ Here, the hydrocarbon fuel burns off the oxide layer (ignition stage), which subsequently allows for the full boron combustion (combustion stage).^{5,8–10} This process elongates the energy release time scale and reduces the total potential energy release of both the boron and hydrocarbon fuel. Theoretical models based on flame test experiments have been developed with the aim to understand the combustion of boron and the removal of the oxide layer. Initially King et al.¹¹ developed a model based on diffusion of molecular oxygen through the oxide layer.^{8,9} Williams et al.^{12–14} and Kuo et al.^{15,16} expanded these boron-based combustion models on the

basis of the rate of boron diffusion through the oxide layer as elucidated by Kuo et al.^{16,17} A comprehensive molecular level gas phase kinetics model incorporating fluorine as an additive was found to inhibit the oxide layer growth.^{18–22} Recently, a model was developed by Pfitzners et al.,^{23,24} this model is derived from the work of Kuo et al.¹⁶ and utilizes generic global reactions in three stages: particle heating without reaction (ignition delay), first stage of combustion (oxide layer removal), and second stage of combustion (clean boron oxidation).

Despite the progress in modeling capabilities, experimental input parameters in B/O/C/H systems, on which the models ultimately rely, has been lacking. As seen in the combustion of hydrocarbons, extensive sets of competing fast radical-mediated reactions have been proposed to occur in combustion environments.^{25,26} Only by investigating each reaction pathway individually can we effectively map out the product branching ratios, reaction mechanisms, and their associated rate constants.

Received: May 27, 2013

Revised: July 19, 2013

Published: July 23, 2013

Boron oxidation is understood to occur sequentially via the reaction $B \rightarrow BO \rightarrow BO_2 \rightarrow B_2O_3$,²⁷ with the formation of the doublet boron monoxide radical as the very first step. For these reasons, our laboratory has started an investigation of elementary reactions of the boronyl radical with a range of unsaturated hydrocarbons using the crossed molecular beams technique.^{28–32} It is important to stress that boron monoxide has been incorporated in the Zhou, Kolb, Rabitz et al. model, and its reaction with molecular hydrogen (H_2) has been previously investigated^{33–35} because of the interest in reactions forming the HOB and HBO molecules; this isomer pair has been deemed to withdraw considerable energy from the boron combustion process. The kinetics of the formation of boron dioxide (BO_2) through the reaction of boron monoxide with molecular oxygen has also been investigated.³³ The reaction was found to occur through atomic oxygen loss and lacked any pressure dependence. In our laboratory, we have investigated under single collision conditions the reactions of boron monoxide (^{11}BO) with acetylene (C_2H_2),³⁶ ethylene (C_2H_4),³⁷ and methylacetylene (CH_3CCH).³⁸ In all cases, the reactions are initiated by the addition of the boron atom of the boron monoxide radical to the π electron density of the unsaturated bond—in the case of methylacetylene via a van der-Waals complex—and proceed via indirect scattering dynamics through the formation of $C_2H_2^{11}BO$, $C_2H_4^{11}BO$, and $C_3H_4^{11}BO$ collision complexes. The latter decompose via atomic hydrogen emission to the $HCC^{11}BO$ (boronyl acetylene), $C_2H_3^{11}BO$ (boronyl ethylene), and $CH_3CC^{11}BO$ (1-propynyl boron monoxide)/ $CH_2CCH^{11}BO$ (propadienyl boron monoxide) products through tight exit transition states. The $C_3H_4^{11}BO$ collision complex also decomposed through the emission of a methyl radical to form $HCC^{11}BO$ (ethynyl boron monoxide). Here, we are expanding these studies and probing the underlying dynamics of the bimolecular gas phase reaction of ground state boron monoxide (^{11}BO ; $X^2\Sigma^+$) with diacetylene (C_4H_2 ; $X^1\Sigma_g^+$) as the simplest representative of the polyynes group. Diacetylene is a typical unsaturated hydrocarbon found in combustion flames in high quantities such as in fuel rich toluene flames with mole fractions of up to 4.4×10^{-3} .³⁹ We will also compare the reaction dynamics of the boron monoxide–diacetylene system with those of the isoelectronic diacetylene–cyano radical (CN ; $X^2\Sigma^+$) system studied earlier in our group.⁴⁰

2. METHODS

2.1. Experimental and Data Analysis. The experiments were carried out under single collision conditions in a crossed molecular beams machine at the University of Hawaii at Manoa.⁴¹ A pulsed supersonic beam of ground state boron monoxide (^{11}BO ; $X^2\Sigma^+$) was produced by laser ablation of a rotating boron rod at 266 nm⁴² while expanding a pulsed beam of carbon dioxide (CO_2 , 99.9999%, BOC) onto the laser ablation zone with a pulsed valve. The beam source is an adaptation of a previous one, employed for C and CN production.^{43,44} The carbon dioxide acts as both a seed and reactant gas to produce boron monoxide most likely by abstraction of an oxygen atom by boron from carbon dioxide. The molecular beam of boron monoxide (^{11}BO ; $X^2\Sigma^+$) seeded in carbon dioxide at a pressure of 4 atm was produced in the primary reaction chamber at a repetition rate of 60 Hz by a pulsed valve operating at -400 V and passed a skimmer and four-slot chopper wheel, to reach the interaction region in the main reaction chamber. The chopper wheel selected a segment

of the boron monoxide (^{11}BO ; $X^2\Sigma^+$) beam with a peak velocity $v_p = 1520 \pm 30$ ms⁻¹ and speed ratio $S = 2.4 \pm 0.3$ (Table 1). A

Table 1. Peak Velocities (v_p), Speed Ratio (S), and the Center-of-Mass Angles (Θ_{CM}), Together with the Nominal Collision Energies (E_{col}) of Diacetylene and Boron Oxide Molecular Beams

	v_p (ms ⁻¹)	S	E_c (kJ mol ⁻¹)	Θ_{CM}
C_4H_2/Ar	620 ± 20	12.0 ± 0.3		
BO/CO_2	1520 ± 7	2.4 ± 0.4	17.5 ± 0.8	39.7 ± 1.7

pulsed valve in the secondary source operated at -500 V generated a pulsed molecular beam of diacetylene (99.5%+) seeded in argon (99.9999%) at fractions of 5% at 550 Torr with a peak velocity $v_p = 620 \pm 20$ ms⁻¹ and speed ratio of 12.0 ± 0.3 (Table 1) that bisected the boron monoxide beam at 90° in the interaction region. Diacetylene was produced using the procedure described previously.⁴⁵ The primary and secondary pulsed valves opened 1890 and 1855 μ s after the time zero as defined by the chopper wheel. The collision energy between the boron monoxide (^{11}BO ; $X^2\Sigma^+$) and diacetylene (C_4H_2 ; $X^1\Sigma_g^+$) was 17.5 ± 0.8 kJ mol⁻¹. Boron has two isotopes, $m/z = 11$ (80%) and $m/z = 10$ (20%), of which the reported collision energy refer to the ^{11}B isotope. Laser induced fluorescence (LIF) was used to characterize the BO radical rovibrational levels. Here, the $A^2\Pi-X^2\Sigma^+$ (0,0) transition at 425 nm was probed *in situ* by a 10 μ J Nd:YAG laser at 10 Hz. The chopper wheel triggered the LIF laser system typically 10 to 20 μ s after the ablation laser fired. The fluorescence was detected by a photomultiplier tube (PMT) and filtered by a 495 nm centered long pass filter for detection of (2,0) fluorescence. The spectra were analyzed using the diatomic spectral simulation program developed by Tan.⁴⁶ The boron monoxide beam was found to have a rotational temperature of $T_{rot} = 250 \pm 40$ K which corresponds to a most probable internal energy of 2.0 ± 0.3 kJ mol⁻¹.⁴⁷ No vibrationally excited boron monoxide radicals were observed.

A rotatable triple differentially pumped quadrupole mass spectrometer (QMS) operating in the time-of-flight (TOF)^{48,49} mode and using electron-impact ionization of about 80 eV was exploited to collect ionized products. By collecting TOF spectra at distinct mass-to-charge (m/z) ratios at intervals of 2.5° over the entire reaction angular distribution of about 40° , a laboratory angular distribution of a distinct mass-to-charge-ratio of the ion was obtained. A forward convolution technique was used to simulate the data in the laboratory frame yielding the center-of-mass translational energy and angular distributions.^{50,51} The product flux contour map, $I(\theta, u) = P(u) \times T(\theta)$, reports the intensity of the reactively scattered products (I) as a function of the center-of-mass scattering angle (θ) and product velocity (u).

2.2. Theoretical Methods. Geometries of various species involved in the reaction of diacetylene with the boron monoxide radical, including the reactants, C_4H_2BO intermediates, transition states, and products, were optimized at the hybrid density functional B3LYP level of theory with the 6-311G(d,p) basis set.^{52,53} Vibrational frequencies and zero-point vibrational energy (ZPE) were obtained using the same B3LYP/6-311G(d,p) approach. The optimized geometries of all species were then used in single-point coupled cluster CCSD(T) calculations^{54–57} (restricted open-shell RHF-RCCSD(T) for open-shell species) with Dunning's correla-

tion-consistent cc-pVDZ, cc-pVTZ, and cc-pVQZ basis sets.⁵⁸ The CCSD(T) total energies were extrapolated to the complete basis set (CBS) limit by fitting the following equation:⁵⁹ $E_{\text{tot}}(x) = E_{\text{tot}}(\infty) + Be^{-Cx}$, where x is the cardinal number of the basis set (2, 3, and 4) and $E_{\text{tot}}(\infty)$ is the CCSD(T)/CBS total energy. B and C are the fitting coefficients of exponential decays of the total energy toward the asymptote, which is the infinite (complete) basis set limit, with basis set expansion.⁵⁹ The Gaussian 09⁶⁰ and MOLPRO 2010⁶¹ programs were used for the ab initio calculations. For some structures, additional CCSD(T)/6-311G(d,p) geometry optimization was carried out employing the ACES II package.⁶²

Rate constants $k(E)$ for unimolecular reaction steps on the C_4H_2BO potential energy surface (PES) were computed using RRKM theory,^{63–65} where the internal energy E was taken as a sum of the energy of chemical activation in the $BO + C_4H_2$ reactions and a collision energy, assuming that a dominant fraction of the latter is converted to the internal vibrational energy. The harmonic approximation was used to calculate the total number and density of states. Product branching ratios were evaluated by solving first-order kinetic equations for unimolecular reactions within the steady-state approximation, according to the kinetics scheme based on the ab initio potential energy diagram. Note that in the calculations of partition functions we apply the harmonic oscillator approximation for the vibrational contribution. To address the most significant anharmonic effects, we treat the appropriate “soft” vibrational modes as internal free or hindered rotations, however, the intermediates considered here do not have such internal rotations. Although a more advanced treatment of anharmonicity may give more accurate results, it is impractically time-consuming for a system of this size. Moreover, according to the literature data, if soft low-frequency modes behaving like hindered rotors are treated anharmonically, but higher frequency modes are treated within the harmonic approximation, the deviations of the calculated rate constants from those obtained using the fully anharmonic treatment do not exceed 30%. Thus, the anharmonicity beyond hindered rotors is expected to have a relatively small effect on rate constants, likely smaller than the anticipated errors of 5 kJ mol^{-1} in reaction barrier heights.

3. RESULTS

3.1. Laboratory Frame. The reactive scattering signal was recorded at mass-to-charge ratios, m/z , of 76 ($C_4H^{11}BO^+$) and 75 ($C_4H^{10}BO^+ / C_4^{11}BO^+$). After scaling, the TOF spectra at $m/z = 76$ and 75 were found to be superimposable indicating that the signal at $m/z = 75$ mainly originates from dissociative ionization of the parent molecule holding a molecular weight of 76 amu (in this respect, it should be noted that the kinematics for the ^{10}BO reaction is slightly different because of the different mass combination, but the effect on the kinematics is much smaller than in the case of the reaction $^{10}B/^{11}B + C_2H_2$).⁶⁶ Hence we can conclude that the $C_4H^{11}BO$ product (76 amu) is formed via the boron monoxide versus hydrogen atom replacement pathway. Note that no signal was observed at $m/z = 52$ ($C_2H^{11}BO^+$) indicating that the boron monoxide versus ethynyl (CCH) exchange channel is closed. Figure 1 depicts selected TOF spectra recorded at $m/z = 76$ ($C_4H^{11}BO^+$). Here, the TOF spectra were fit with a single channel fit with a mass combination of 76 amu ($C_4H^{11}BO^+$) and 1 amu (H^+). The TOF spectra at each angle were also integrated and scaled by the number of scans taken and by the fluctuating beam

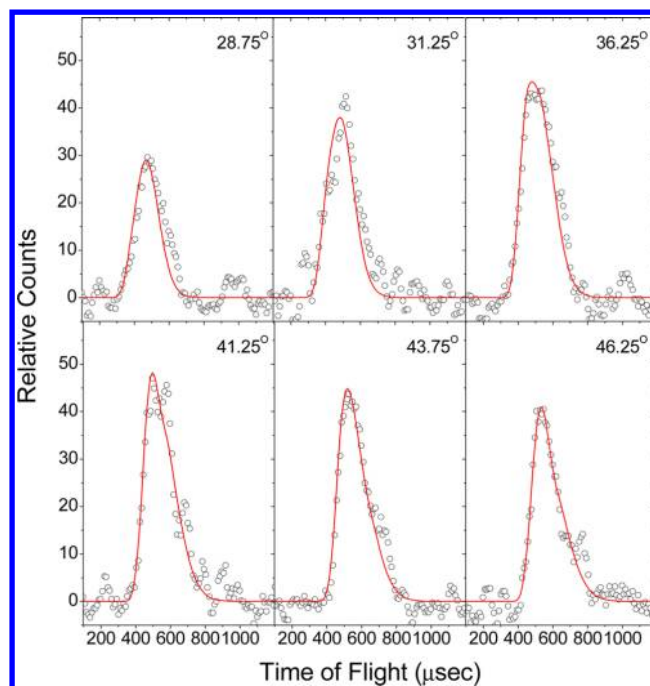


Figure 1. Time-of-flight data at various laboratory angles recorded at $m/z = 76$ for the reaction of boron monoxide (^{11}BO ; $X^2\Sigma^+$) with diacetylene (C_4H_2 ; $X^1\Sigma_g^+$) at a collision energy of $17.5 \pm 0.8 \text{ kJ mol}^{-1}$. The circles indicate the experimental data, and the solid lines indicate the calculated fits.

intensities to derive the laboratory angular distribution (LAB) of the $C_4H^{11}BO$ product at $m/z = 76$ (Figure 2). The

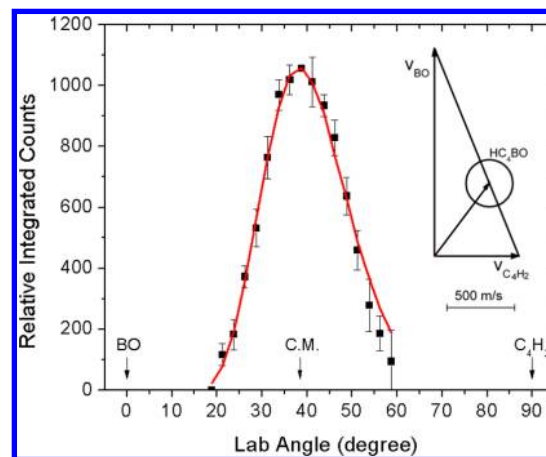


Figure 2. Laboratory angular distribution (LAB) of the $C_4H^{11}BO$ isomer(s) at $m/z = 76$ formed in the reaction of boron monoxide (^{11}BO ; $X^2\Sigma^+$) with diacetylene (C_4H_2 ; $X^1\Sigma_g^+$) at a collision energy of $17.5 \pm 0.8 \text{ kJ mol}^{-1}$. Circles and error bars indicate experimental data, and the solid line indicates the calculated distribution.

laboratory angular distribution peaks at $38.8^\circ \pm 0.5^\circ$ close to the center-of-mass angle of $39.6^\circ \pm 1.5^\circ$ and extends by about 40° in the scattering plane as defined by the primary and secondary beams. The peaking at the center-of-mass angle and nearly symmetric profile suggest that the reaction proceeds through indirect (complex forming) scattering dynamics involving $C_4H_2^{11}BO$ reaction intermediate(s).

3.2. Center-of-Mass Frame. Having established the presence of a boron monoxide versus atomic hydrogen

exchange and the formation of a molecule with the molecular formula $C_4H^{11}BO$ (76 amu), we now attempt to elucidate the underlying reaction dynamics by converting the laboratory data into the center-of-mass frame using a forward convolution routine. This provides the center-of-mass translational energy ($P(E_T)$) and angular ($T(\theta)$) distributions (Figure 3). Here, a

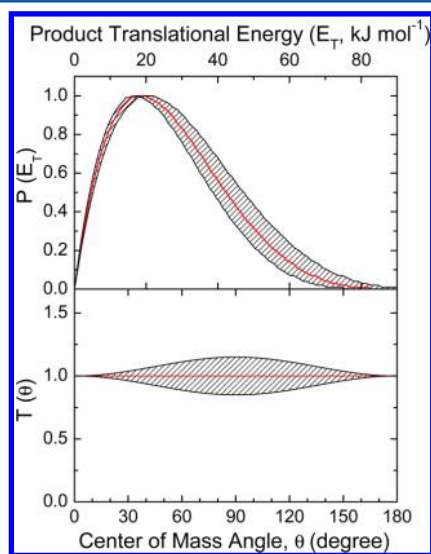


Figure 3. Center-of-mass translational energy distribution (top) and angular distribution (bottom) for the reaction of boron monoxide (^{11}BO ; $X^2\Sigma^+$) with diacetylene (C_4H_2 ; $X^1\Sigma_g^+$) to form boronyldiacetylene ($HCCCC^{11}BO$) and atomic hydrogen at a collision energy of 17.5 ± 0.8 kJ mol^{-1} .

single channel fit with a center-of-mass translational energy distribution, $P(E_T)$, exposing a maximum translational energy release of 82 ± 10 kJ mol^{-1} , furnishes the best fit of the laboratory data. From this fit, the reaction exoergicity can be calculated for those products born without internal energy by subtracting the collision energy (17.5 ± 0.8 kJ mol^{-1}) from the maximum translational energy of 82 ± 10 kJ mol^{-1} . Therefore, we find the reaction exoergicity to be 64.5 ± 10.6 kJ mol^{-1} in forming the $C_4H^{11}BO$ isomer(s) plus atomic hydrogen if the reactants have no rovibrational excitation. Considering further the most probable internal energy of the boron monoxide

reactant of 2.0 ± 0.3 kJ mol^{-1} (section 2.1), the reaction energy is reduced to 62.5 ± 10.9 kJ mol^{-1} . Further, the $P(E_T)$ depicts a flux distribution peaking away from zero translational energy at about $15\text{--}22$ kJ mol^{-1} suggesting that at least one reaction channel to form the $C_4H^{11}BO$ isomer(s) plus atomic hydrogen could hold a tight exit transition state and involves a repulsive carbon–hydrogen bond rupture with a significant electron rearrangement. The center-of-mass translational energy distribution $P(E_T)$ further portrays that the average amount of energy released into the translational degrees of freedom of the products is 27 ± 5 kJ mol^{-1} , which is $33 \pm 6\%$ of the total available energy. In addition, the center-of-mass angular distribution, $T(\theta)$, provides important information on the scattering dynamics. This distribution shows intensity over the whole angular range, which is indicative of an indirect, complex-forming reaction mechanism involving $C_4H^{11}BO$ intermediate(s).⁶⁷ The center-of-mass angular distribution is also forward–backward symmetric as well as isotropic; this finding suggests that the lifetime (τ) of the decomposing complex is longer than its rotational period. The isotropy of the center-of-mass angular distribution indicates a weakly polarized system suggesting that the initial orbital angular momentum does not couple well with the final orbital angular momentum. This occurs because the light hydrogen atom cannot carry away much orbital angular momentum. Most of the initial angular momentum is therefore channeled into the rotational degrees of freedom of the $C_4H^{11}BO$ product isomer(s).⁶⁷ The above characteristics can be also visualized in the flux contour map (Figure 4).

3.3. Theoretical Results. The theoretically calculated reaction pathways and associated intermediate as well as transition states in the reaction of boron monoxide with diacetylene are illustrated in Figure 5 and their molecular structures are illustrated in Figure 6. First, we will consider only those reaction pathways which are open at the experimental collision energy of 17.5 kJ mol^{-1} ; these pathways can be found below the red dashed line inserted in the PES. All intermediates, transition states, and products above this line are not accessible from the energetical standpoint and hence are discussed later. With its radical center localized on the boron atom, the boronyl radical (^{11}BO) adds to the π orbital of the diacetylene molecule at one of the terminal carbon atoms without an entrance barrier leading to intermediate **i1** ($C_4H_2^{11}BO$), which is stabilized by

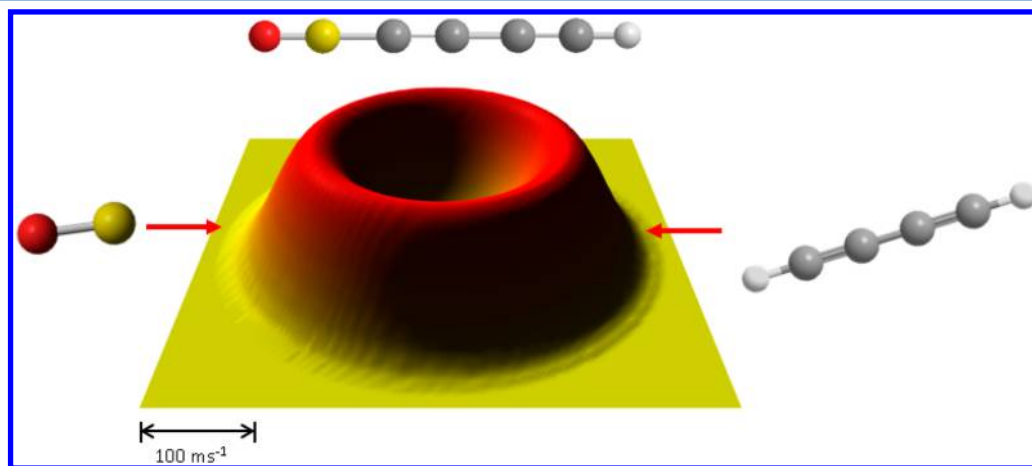


Figure 4. Flux contour map of the reaction of boron monoxide (^{11}BO ; $X^2\Sigma^+$) with diacetylene (C_4H_2 ; $X^1\Sigma_g^+$) forming the boronyldiacetylene ($C_4H^{11}BO$) molecule and atomic hydrogen at a collision energy of 17.5 ± 0.8 kJ mol^{-1} .

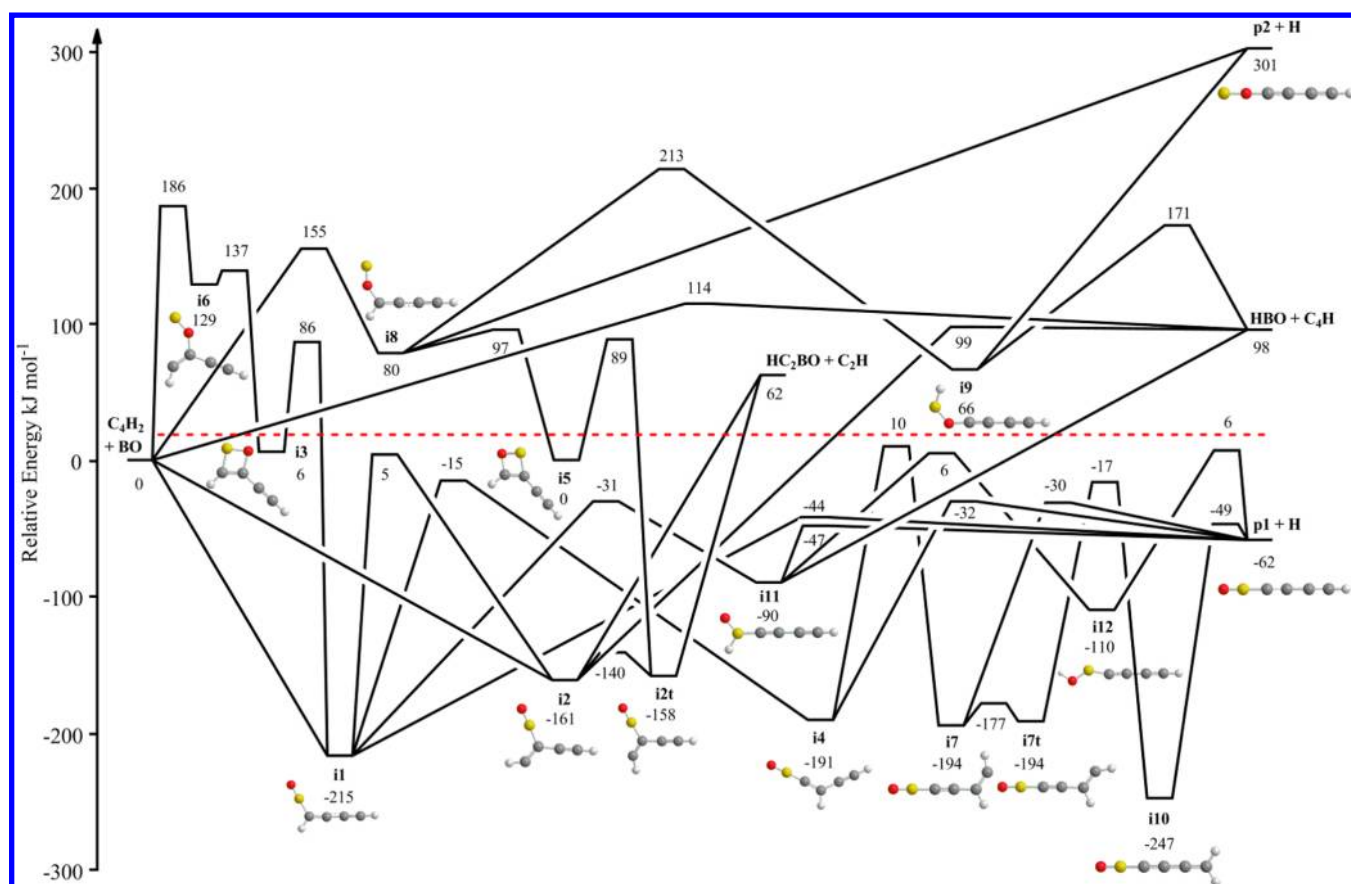


Figure 5. Schematic representation of the doublet $C_4H_2^{11}BO$ potential energy surface (PES) accessed via the reaction of boron monoxide (^{11}BO ; $X^2\Sigma^+$) with diacetylene (C_4H_2 ; $X^1\Sigma_g^+$). The red dashed line represents the collision energy in our experiments; all stationary points above that line are therefore experimentally not accessible.

215 kJ mol^{-1} with respect to the separated reactants. We neither located a transition state nor a van der Waals complex between the boron monoxide radical and the diacetylene molecule in the entrance channel to the **i1** adduct at the B3LYP/6-311G(d,p) or CCSD(T)/6-311G(d,p) levels of theory. From **i1** hydrogen emission can occur from the C1 carbon atom to reach the products **p1** ($HCCCC^{11}BO$) plus atomic hydrogen by overcoming 171 kJ mol^{-1} via a tight exit transition state located 18 kJ mol^{-1} above the separated products. The formation of **p1** ($HCCCC^{11}BO$) plus atomic hydrogen is exoergic by 62 kJ mol^{-1} and represents the *only* exoergic product available on the $C_4H_2^{11}BO$ potential energy surface. The reaction from the reactants through **i1** and forming **p1** holds the least steps and can be classified as an addition–elimination pathway. Interestingly, the structure of **p1** appears to be slightly nonlinear at the B3LYP/6-311G(d,p) level of theory, with the largest deviation from the linearity of 3.3° observed for the CCB angle. However, geometry optimization at the CCSD(T)/6-311G(d,p) level gives a linear geometry. The discrepancies in the bond lengths computed at the B3LYP and CCSD(T) levels do not exceed 0.02 \AA (see Figure 6), whereas the CCSD(T)/CBS total energy of **p1** calculated with the CCSD(T)/6-311G(d,p) optimized geometry is 3 kJ mol^{-1} lower than that with the B3LYP/6-311G(d,p) structure.

Our calculations also exposed five alternative reaction pathways to **p1** that shall now be described. From the initial collision complex **i1**, the hydrogen on the C1 carbon atom can migrate to the C2 carbon by overcoming a significant barrier of 200 kJ mol^{-1} to reach intermediate **i4** located 191 kJ mol^{-1}

below the reactants. The products **p1** ($HCCCC^{11}BO$) can be accessed from **i4** through emission of the hydrogen atom from the C2 carbon atom. The hydrogen emission from **i4** involves a tight exit transition state placed 30 kJ mol^{-1} above the separated reactants. Intermediate **i4** can also isomerize to **i7**, which is located 194 kJ mol^{-1} below the reactants through another hydrogen shift from C2 to C3 by overcoming a 201 kJ mol^{-1} barrier. From this intermediate, the products **p1** ($HCCCC^{11}BO$) can also be formed through hydrogen emission from the C3 carbon by passing through a tight exit transition state located 32 kJ mol^{-1} above the products. Intermediate **i7** can also isomerize to its trans form over a small barrier of only 17 kJ mol^{-1} to reach intermediate **i7t**. From here, this intermediate undergoes yet another hydrogen shift to **i10**; the latter represents the global potential minimum of this PES and is located 247 kJ mol^{-1} below the separated reactants. Finally, intermediate **i10** emits a hydrogen atom from the terminal carbon atom to reach the product **p1** ($HCCCC^{11}BO$) via a tight exit transition state located 13 kJ mol^{-1} above the products. Further, after forming the initial intermediate **i1**, the hydrogen atom on the C1 carbon atom can also migrate in the opposite direction to the boron atom by overcoming a 184 kJ mol^{-1} barrier to reach intermediate **i11** located 90 kJ mol^{-1} below the separated reactants. Intermediate **i11** can emit a hydrogen atom located on the boron atom to reach the product **p1** ($HCCCC^{11}BO$) via an exit barrier of 15 kJ mol^{-1} . Alternatively, intermediate **i11** can undergo a final hydrogen migration from the boron to the oxygen atom over a 96 kJ mol^{-1} barrier to reach intermediate **i12** located 110 kJ mol^{-1}

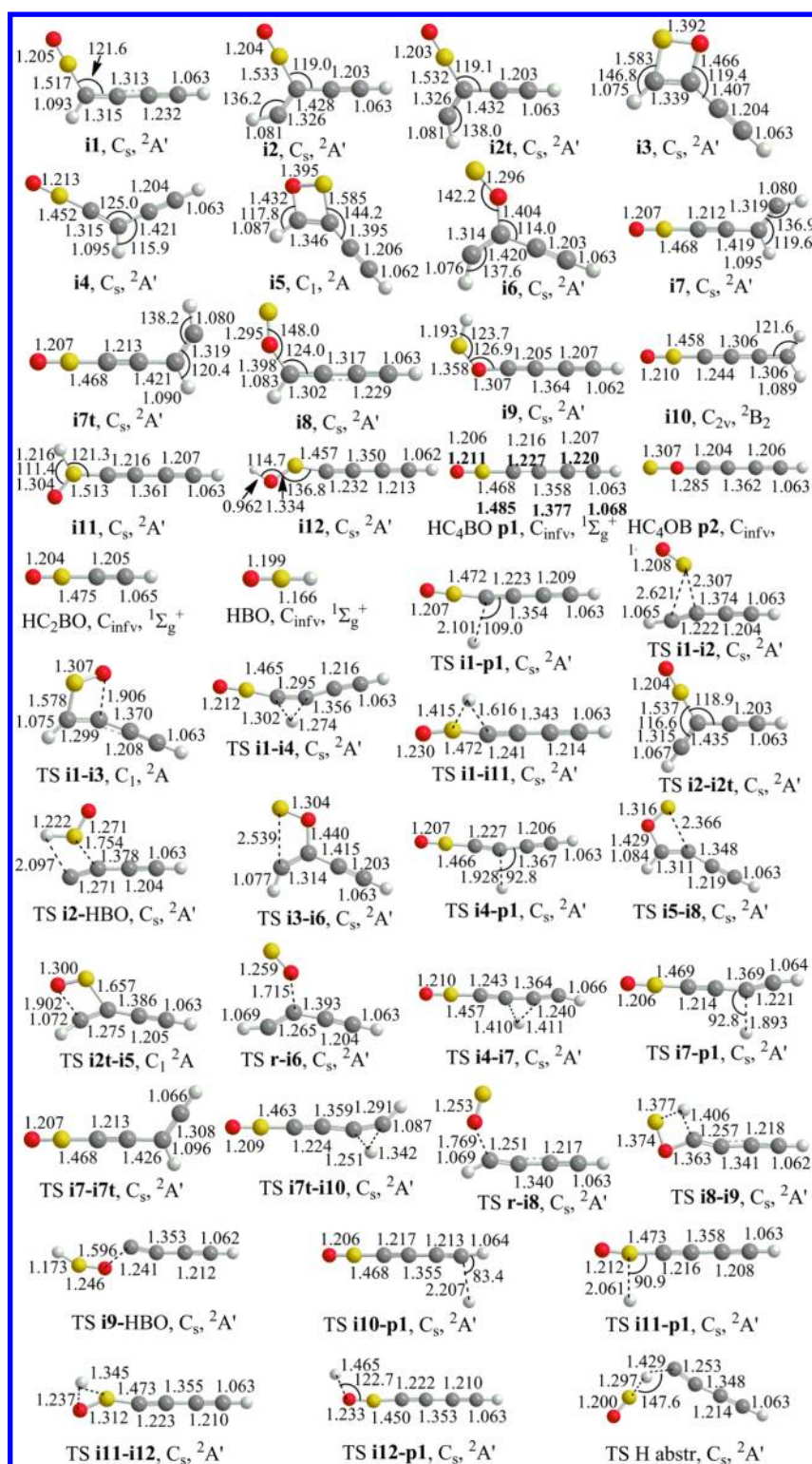


Figure 6. Structures of stationary points (intermediates, transition states, products) on the $C_4H_2^{11}BO$ potential energy surface (PES) calculated at the B3LYP/6-311G(d,p) level of theory (the parameters for HC_4BO **p1** computed at the CCSD(T)/6-311G(d,p) level are given in bold). The numbers show bond lengths in Å and bond angles in degrees.

below the energy of the reactants. The product **p1** ($HCCCC^{11}BO$) is accessed from **i12** by emission of a hydrogen atom from the oxygen atom by passing through a tight exit transition state located 68 kJ mol^{-1} above the products. It should also be noted intermediate **i11** can dissociate along the boron carbon bond to reach the HBO

plus CCCCH products in an overall endoergic reaction ($+98 \text{ kJ mol}^{-1}$).

We will now discuss the remaining reaction pathways leading to products that are energetically inaccessible under our experimental conditions. The initial intermediate **i1** can undergo a boronyl migration from the C1 to the C2 carbon

atom over a barrier of 220 kJ mol⁻¹ to reach intermediate **i2** located 161 kJ mol⁻¹ below the reactants. Intermediate **i2** can undergo a hydrogen migration from the C1 carbon to the boron atom and subsequently dissociate along the oxygen–carbon bond to reach the products HBO + C₄H in an overall endoergic reaction (+98 kJ mol⁻¹). Alternatively, intermediate **i2** can dissociate along the C2–C3 carbon bond to reach the products HCC¹¹BO plus the ethynyl radical (C₂H) placed 62 kJ mol⁻¹ above the energy of the reactants. Intermediate **i2** can also isomerize to **i2t** located in a potential energy well of 158 kJ mol⁻¹; this intermediate can undergo cyclization by forming a bond between the oxygen atom and the terminal C1 carbon atom to reach intermediate **i5**; however, the associated barrier of 89 kJ mol⁻¹ (relative to the initial reactants) cannot be overcome under our experimental conditions. From **i2t**, a similar C2–C3 carbon bond rupture as in **i2** can occur to reach the products HCC¹¹BO plus the ethynyl radical (C₂H). The ¹¹BO reactant can also directly abstract a hydrogen atom from diacetylene over a barrier of 114 kJ mol⁻¹ to reach the products HBO plus HCCCC. Alternatively, ¹¹BO can bind to the C1 carbon of diacetylene with its oxygen atom—a process that must surmount a considerable barrier of 155 kJ mol⁻¹ leading to intermediate **i8** located 80 kJ mol⁻¹ above the reactants. Intermediate **i8** can emit a hydrogen atom from the C1 carbon to reach the product **p2** HCCCCO¹¹B located at an energy of 301 kJ mol⁻¹ above the separated reactants. Intermediate **i8** alternatively can form a tetracyclic ring structure **i5** through binding of the boron atom to the C2 carbon atom by overcoming a small barrier of only 17 kJ mol⁻¹. The last option for intermediate **i8** involves a hydrogen migration from the C1 carbon atom to the terminal boron atom to access intermediate **i9**. The latter can form the products HBO plus HCCCC through cleavage of the oxygen–carbon bond. Intermediate **i9** can also emit a hydrogen atom from the boron atom to reach the product **p2** HCCCCO¹¹B. Finally, a bonding of the oxygen atom to the C2 carbon of diacetylene has been identified; this pathway involves an entrance barrier of 186 kJ mol⁻¹ and reaches intermediate **i6** located 129 kJ mol⁻¹ above the energy of the separated reactants. Here, intermediate **i6** can form a tetracyclic structure (intermediate **i3**) by bonding of the boron atom and the C1 carbon atom via a barrier of 8 kJ mol⁻¹. The formation of **i3** will lead to a ring-opening by breaking the oxygen–carbon bond to reach the initial intermediate **i1**.

To aid in deciphering the reaction pathway computationally, we first eliminate all intermediates, transition states, and products which are energetically not accessible under our experimental conditions, that is, those located above the “dashed red line” in Figure 5. Considering the remaining stationary points, RRKM theory was exploited to calculate the branching ratios for the formation of the product **p1** (HCCCC¹¹BO) plus atomic hydrogen via five distinct reaction paths starting from intermediate **i1**. These calculations predict that at our collision energy of 17.5 kJ mol⁻¹, about 94% of **p1** originates from **i1**, whereas only about 5% is formed after isomerization of **i1** to **i11** (Table 2).

4. DISCUSSION

4.1. Product Identification. We now combine our electronic structure calculations with the results from the crossed molecular beams studies to rationalize the product(s) formed in the system under study. The experimental data suggest the formation of a product with the molecular formula C₄H¹¹BO formed via a ¹¹BO versus hydrogen atom exchange

Table 2. Calculated Branching Ratios (%) for the Formation of **p1 from Various Intermediates in the Reaction of Boronyl Radicals with Diacetylene**

	<i>E</i> _{coll} kJ mol ⁻¹					
	0	4.18	8.37	12.55	17.50	20.92
from i1	95.97	95.53	95.10	94.68	94.20	93.89
from i11	3.62	3.97	4.30	4.61	4.95	5.17
from i12	0.00	0.00	0.00	0.00	0.00	0.00
from i4	0.41	0.50	0.60	0.71	0.85	0.95
from i7	0.00	0.00	0.00	0.00	0.00	0.00
from i10	0.00	0.00	0.00	0.00	0.00	0.00

mechanism. No molecular hydrogen loss pathway has been observed. Further, the reaction energy was determined experimentally to be 62.5 ± 10.9 kJ mol⁻¹; these energetics correlate nicely with the computed reaction energy to form product **p1** (HCCCC¹¹BO) plus atomic hydrogen (−62 ± 5 kJ mol⁻¹). Isomer **p2** (HCCCCO¹¹B) is energetically not accessible since its formation is endothermic by 301 kJ mol⁻¹. Therefore, we can conclude that the reaction of the boronyl radical with diacetylene leads to the formation of the hitherto elusive boronyldiacetylene molecule (HCCCC¹¹BO; X¹Σ⁺) under single collision conditions.

4.2. Proposed Reaction Dynamics. Having identified the reaction products to be boronyldiacetylene (HCCCC¹¹BO; X¹Σ⁺) plus atomic hydrogen, we propose the following reaction dynamics. A comparison of the molecular structures of the reactants with the boronyldiacetylene product indicates that the hydrogen atom in diacetylene is effectively replaced by the ¹¹BO group. Here, the ¹¹BO radical adds with the radical centered on the boron atom to the C1 carbon atom of the diacetylene molecule forming intermediate **i1**. The indirect (complex forming) nature of the reaction was also inferred experimentally based on the center-of-mass angular distribution depicting intensity over the full angular range. All other addition steps result in reaction pathways that lead to energetically inaccessible products such as **p2**. From **i1**, hydrogen emission from the C1 carbon atom leads to the products boronyldiacetylene (HCCCC¹¹BO) plus atomic hydrogen through a tight exit transition state (18 kJ mol⁻¹); the theoretically predicted tight exit transition state matches the experimental prediction of a tight exit transition state located about 15 to 22 kJ mol⁻¹ above the separated products. Recall that the theoretical calculated branching ratios support these conclusions. Here, the formation of boronyldiacetylene plus atomic hydrogen is found to occur with a branching ratio of about 95% from intermediate **i1**. The next closest contender forms the products **p1** plus atomic hydrogen with a branching ratio of about 5% through isomerization from intermediate **i1** to **i11** which involves a hydrogen migration from C1 to the boron atom followed by hydrogen emission from the boron atom. It should be noted that the formation of **i11** from **i1** involves the surmounting of a barrier that is 13 kJ mol⁻¹ higher than the exit transition state associated with hydrogen emission from **i1** to form boronyldiacetylene; this might explain the low branching ratio of **p1** formation from **i11**.

4.3. Comparison to the Isoelectronic Cyano Radical Reaction. We shall now compare the reaction of boron monoxide (BO) with diacetylene to the reaction of the isoelectronic cyano radical (CN) studied previously in our laboratory.⁴⁰ Boron monoxide (BO) and the cyano radical (CN) are isoelectronic and can both be considered as

pseudohalogen because of their high electron affinity.⁶⁸ Indeed, both systems undergo defacto hydrogen atom–radical exchange mechanisms via complex formation forming linear products cyanodiacetylene (HCCCCCN) and boronyldiacetylene (HCCCC¹¹BO) in overall exoergic reactions of 87 ± 15 kJ mol⁻¹ and 64.5 ± 10.6 kJ mol⁻¹, respectively. The reaction mechanism extracted in both systems are identical: in the cyano reaction, the radical bearing carbon atom binds to the C1 carbon of diacetylene to reach the initial intermediate **i1** bound by about 200 kJ mol⁻¹ relative to the reactants similarly to the boron monoxide study (intermediate **i1** is bound by 215 kJ mol⁻¹). Both intermediates decompose via tight exit transition states located about 15 to 20 kJ mol⁻¹ above the separated products. All intermediates, transition states, and exit transition states relevant to the formation of the final products under single collision conditions have comparable energies and structures.

5. SUMMARY

The reaction of the boron monoxide radical with diacetylene was investigated at a collision energy of 17.5 kJ mol⁻¹ employing the crossed molecular beam technique and supported by *ab initio* and RRKM calculations. The reaction shows indirect scattering dynamics via complex formation, which produces the hitherto elusive boronyldiacetylene product (HCCCC¹¹BO) via a tight exit transition state. The reaction is initiated by a barrierless addition of the boron atom in the ¹¹BO radical to the terminal C1 carbon atom of the diacetylene molecule forming a C₄H₂¹¹BO reaction intermediate. Although several reaction pathways exist to the ultimate boronyldiacetylene product, the most efficient reaction pathway from the initial collision complex **i1** to the final products (**p1** plus atomic hydrogen) is found to be taken as supported by the RRKM theory (95%). Combustion environments of hydrocarbons often contain an abundance of diacetylene, and in the combustion of boron, the boron monoxide radical is initially produced. With the presence of the reactants to the title reaction in combustion environments involving boron and hydrocarbons such as rocket propellants we can anticipate the facile formation of boronyldiacetylene through single bimolecular collisions. The formation of boronyldiacetylene described here adds to the growing knowledge of B/O/C/H reactions studied such as those involving boron monoxide and ethylene³² and acetylene.³¹ The isoelectronic character between boron monoxide and the cyano radical in reaction with unsaturated hydrocarbons is prevalent here in the reaction with diacetylene demonstrated with similar reaction dynamics and potential energy surfaces. From these continuing studies we can expect a deep understanding of the role of boron monoxide in boron combustion in hydrocarbon fuels.

■ ASSOCIATED CONTENT

Supporting Information

Cartesian coordinates (Å), rotational constants (GHz), and vibrational frequencies (cm⁻¹) of various intermediates and products involved in the BO + C₄H₂ reaction calculated at the B3LYP/6-311G(d,p) level (also at the CCSD(T)/6-311G(d,p) level for C₄HBO **p1**). This material is available free of charge via the Internet at <http://pubs.acs.org>.

■ AUTHOR INFORMATION

Corresponding Author

*

Notes

The authors declare no competing financial interest.

†Permanent Address: (N.B.) Dipartimento di Chimica, University of Perugia, Perugia, Italy.

‡Permanent Address: (D.S.) Dipartimento di Chimica, Università La Sapienza, Rome, Italy.

■ ACKNOWLEDGMENTS

This work was supported by the Air Force Office of Scientific Research (FA9550-12-1-0213).

■ REFERENCES

- (1) Osmont, A.; Gokalp, I.; Catoire, L. Evaluating Missile Fuels. *Propellants, Explos., Pyrotech.* **2006**, *31*, 343–354.
- (2) Edwards, T. Liquid Fuels and Propellants for Aerospace Propulsion: 1903–2003. *J. Propul. Power* **2003**, *19*, 1089–1107.
- (3) Hinchey, J. J. Kinetics for the Quenching and Relaxation of Boron Oxide. *J. Chem. Phys.* **1993**, *99*, 4403–4410.
- (4) King, M. K. Ignition and Combustion of Boron Particles and Clouds. *J. Spacecraft Rockets* **1982**, *19*, 294.
- (5) Antaki, P.; Williams, F. A. Observations on the Combustion of Boron Slurry Droplets in Air. *Combust. Flame* **1987**, *67*, 1–8.
- (6) Li, S. C.; Williams, F. A. *Combustion of Boron-Based Solid Propellants and Solid Fuels*; CRC Press: Boca Raton, FL, 1993; p 248.
- (7) Turns, S. R.; Holl, J. T.; Solomon, A. S. P.; Faeth, G. M. Gasification of Boron Oxide Drops in Combustion Gases. *Combust. Sci. Technol.* **1985**, *43*, 287–300.
- (8) Macek, A.; Semple, J. M. *Combustion of Boron Carbide Particles*; Atl. Res. Div., Susquehanna Corp.: Alexandria, VA, USA, 1971.
- (9) Macek, A.; Semple, J. M. Combustion of Boron Particles at Atmospheric Pressure. *Combust. Sci. Technol.* **1969**, *1*, 181–191.
- (10) Yuasa, S.; Yoshida, T.; Kawashima, M.; Isoda, H. Effects of Pressure and Oxygen Concentration on Ignition and Combustion of Boron in Oxygen/Nitrogen Mixture Streams. *Combust. Flame* **1998**, *113*, 380–387.
- (11) King, M. K. *Combust. Sci. Technol.* **1972**, *5*, 155–164.
- (12) Mohan, G.; Williams, F. A. Ignition and Combustion of Boron in Oxygen/Inert Atmosphere. *Am. Inst. Aeronaut. Astronaut. J.* **1972**, *108*, 776–783.
- (13) Li, S. C.; Williams, F. A. Ignition and Combustion of Boron in Wet and Dry Atmospheres, *Symp. (Int.) Combust., [Proc.]*, **1991**, *23rd*, 1147–1154.
- (14) Li, S. C. Optical Measurement of Size Histories of Boron Particles in Ignition and Combustion Stages. *Combust. Sci. Technol.* **1991**, *77*, 149–169.
- (15) Yeh, C. L.; Kuo, K. K. Theoretical Model Development and Verification of Diffusion/Reaction Mechanisms of Boron Particle Combustion, Transport Phenomena in Combustion. Proceedings of the International Symposium on Transport Phenomena in Combustion, 8th, San Francisco, July 16–20, 1995; Taylor & Francis: Oxford, UK, 1996; Vol. 1, pp 45–63.
- (16) Yeh, C. L.; Kuo, K. K. Ignition and Combustion of Boron Particles. *Prog. Energy Combust. Sci.* **1997**, *22*, 511–541.
- (17) Yeh, C. L.; Kuo, K. K. Experimental Studies of Boron Particle Combustion, Transport Phenomena in Combustion, Proceedings of the International Symposium on Transport Phenomena in Combustion, 8th, San Francisco, July 16–20, 1995; Taylor & Francis: Oxford, UK, 1996; Vol. 2, pp 1461–1472.
- (18) Brown, R. C.; Kolb, C. E.; Cho, S. Y.; Yetter, R. A.; Dryer, F. L.; Rabitz, H. Kinetic Model for Hydrocarbon-Assisted Particulate Boron Combustion. *Int. J. Chem. Kinetics* **1994**, *26*, 319–332.
- (19) Brown, R. C.; Kolb, C. E.; Yetter, R. A.; Dryer, F. L.; Rabitz, H. Kinetic Modeling and Sensitivity Analysis for B/H/O/C/F Combination Systems. *Combust. Flame* **1995**, *101*, 221–238.
- (20) Zhou, W.; Yetter, R. A.; Dryer, F. L.; Rabitz, H.; Brown, R. C.; Kolb, C. E. Effect of Fluorine on the Combustion of “Clean” Surface Boron Particles. *Combust. Flame* **1998**, *112*, 507–521.

- (21) Zhou, W.; Yetter, R. A.; Dryer, F. L.; Rabitz, H.; Brown, R. C.; Kolb, C. E. Ignition and Combustion of Boron Particles in Fluorine Containing System. *Chem. Phys. Proc. Combust.* **1996**, 495–498.
- (22) Zhou, W.; Yetter, R. A.; Dryer, F. L.; Rabitz, H.; Brown, R. C.; Kolb, C. E. Multi-Phase Model for Ignition and Combustion of Boron Particles. *Combust. Flame* **1999**, *117*, 227–243.
- (23) Hussmann, B.; Pfitzner, M. Extended Combustion Model for Single Boron Particles. Part II: Validation, *Combust. Flame*, *157*, 822–833.
- (24) Hussmann, B.; Pfitzner, M. Extended Combustion Model for Single Boron Particles. Part I: Theory, *Combust. Flame*, *157*, 803–821.
- (25) Kaiser, R. I.; Mebel, A. M. The Reactivity of Ground-State Carbon Atoms with Unsaturated Hydrocarbons in Combustion Flames and in the Interstellar Medium. *Int. Rev. Phys. Chem.* **2002**, *21*, 307–356.
- (26) Kaiser, R. I.; Le, T. N.; Nguyen, T. L.; Mebel, A. M.; Balucani, N.; Lee, Y. T.; Stahl, F.; Schleyer, P. v. R.; Schaefer, H. F., III. A Combined Crossed Molecular Beam and ab Initio Investigation of C2 and C3 Elementary Reactions with Unsaturated Hydrocarbons—Pathways to Hydrogen Deficient Hydrocarbon Radicals in Combustion Flames. *Faraday Discuss.* **2001**, *119*, 51–66.
- (27) Bauer, S. H. Oxidation of B, BH, BH₂, and B_mH_n Species: Thermochemistry and Kinetics. *Chem. Rev.* **1996**, *96*, 1907–1916.
- (28) Balucani, N.; Zhang, F.; Kaiser, R. I. Elementary Reactions of Boron Atoms with Hydrocarbons—Toward the Formation of Organo-Boron Compounds. *Chem. Rev.* **2010**, *110*, 5107–5127.
- (29) Balucani, N.; Asvany, O.; Lee, Y. T.; Kaiser, R. I.; Galland, N.; Hannachi, Y. Observation of Borirene from Crossed Beam Reaction of Boron Atoms with Ethylene. *J. Am. Chem. Soc.* **2000**, *122*, 11234–11235.
- (30) Kaiser, R. I.; Balucani, N.; Galland, N.; Caralp, F.; Rayez, M. T.; Hannachi, Y. Unraveling the Chemical Dynamics of Bimolecular Reactions of Ground State Boron Atoms, B(²P₁), with Acetylene, C₂H₂. *Phys. Chem. Chem. Phys.* **2004**, *6*, 2205–2210.
- (31) Zhang, F.; Gu, X.; Kaiser, R. I.; Balucani, N.; Huang, C. H.; Kao, C. H.; Chang, A. H. H. A Crossed Beam and ab Initio Study of the Reaction of Atomic Boron with Ethylene. *J. Phys. Chem. A* **2008**, *112*, 3837–3845.
- (32) Maksyutenko, P.; Zhang, F.; Kim, Y. S.; Kaiser, R. I.; Chen, S. H.; Wu, C. C.; Chang, A. H. H. Untangling the Chemical Dynamics of the Reaction of Boron Atoms, ¹¹B(²P₁), with Diacetylene, C₄H₂(X¹Σ_g⁺)—A Crossed Molecular Beams and ab Initio Study. *J. Phys. Chem. A* **2010**, *114*, 10936–10943.
- (33) Garland, N. L.; Stanton, C. T.; Nelson, H. H.; Page, M. Temperature Dependence of the Kinetics of the Reaction Boron Monoxide + Hydrogen → Oxoborane + Atomic Hydrogen. *J. Chem. Phys.* **1991**, *95*, 2511–2515.
- (34) Page, M. *Multireference Configuration Interaction Study of the Reaction: Molecular Hydrogen + Boron Oxide (BO) Yields Atomic Hydrogen + Hydrogen Boride Oxide (HBO)*; Nav. Res. Lab.: Washington, DC, USA, 1988.
- (35) Chin, C.-H.; Mebel, A. M.; Hwang, D.-Y. Theoretical Study of the Reaction Mechanism of BO, B₂O₂, and BS with H₂. *J. Phys. Chem. A* **2004**, *108*, 473–483.
- (36) Parker, D. S. N.; Zhang, F.; Maksyutenko, P.; Kaiser, R. I.; Chang, A. H. H. A Crossed Beam and ab Initio Investigation of the Reaction of Boron Monoxide (BO) with Acetylene (C₂H₂). *Phys. Chem. Chem. Phys.* **2011**, *13*, 8560–8570.
- (37) Parker, D. S. N.; Zhang, F.; Maksyutenko, P.; Kaiser, R. I.; Chen, S. H.; Chang, A. H. H. A Crossed Beam and ab Initio Investigation on the Formation of Vinyl Boron Monoxide (C₂H₃BO) via Reaction of Boron Monoxide (BO) with Ethylene (C₂H₄). *Phys. Chem. Chem. Phys.* **2012**, *14*, 11099–11106.
- (38) Maity, S.; Parker, D. S. N.; Dangi, B. B.; Kaiser, R. I.; Fau, S.; Rerera, A.; Bartlett, R. J. *J. Phys. Chem. A* **2013**, DOI: 10.1021/jp402743y.
- (39) Li, Y.; Zhang, L.; Tian, Z.; Yuan, T.; Wang, J.; Yang, B.; Qi, F. An Experimental Study of a Fuel-Rich Premixed Toluene Flame at Low Pressure. *Energy Fuels* **2009**, *23*, 1473–1485.
- (40) Zhang, F.; Kim, S.; Kaiser, R. I.; Jamal, A.; Mebel, A. M. A Crossed Beams and ab Initio Investigation on the Formation of Cyanodiacetylene in the Reaction of Cyano Radicals with Diacetylene. *J. Chem. Phys.* **2009**, *130*, 234308/1.
- (41) Gu, X.; Guo, Y.; Zhang, F.; Mebel, A. M.; Kaiser, R. I. Reaction Dynamics of Carbon-Bearing Radicals in Circumstellar Envelopes of Carbon Stars. *Faraday Discuss.* **2006**, *133*, 245.
- (42) Gu, X.; Guo, Y.; Kawamura, E.; Kaiser, R. I. Characteristics and Diagnostics of an Ultrahigh Vacuum Compatible Laser Ablation Source for Crossed Molecular Beam Experiments. *J. Vac. Sci. Technol., A* **2006**, *24*, 505–511.
- (43) Kaiser, R. I.; Suits, A. G. A High-Intensity, Pulsed Supersonic Carbon Source with C(³P₁) Kinetic Energies of 0.08–0.7 eV for Crossed Beam Experiments. *Rev. Sci. Instrum.* **1995**, *66*, 5405–5411.
- (44) Kaiser, R. I.; Ting, J. W.; Huang, L. C. L.; Balucani, N.; Asvany, O.; Lee, Y. T.; Chan, H.; Stranges, D.; Gee, D. A Versatile Source to Produce High-Intensity, Pulsed Supersonic Radical Beam for Crossed-Beams Experiments: The Cyanogen Radical CN(X²Σ⁺) as a case study. *Rev. Sci. Instrum.* **1999**, *70*, 4185–4191.
- (45) Zhang, F.; Kim, S.; Kaiser, R. I.; Mebel, A. M. On the Formation of the 1,3,5-Hexatrienyl Radical (C₆H(X²Π)) via the Crossed Beams Reaction of Dicarbon (C₂(X¹Σ_g⁺/a³Π_u)), with Diacetylene (C₄H₂(X²Π)). *J. Phys. Chem. A* **2009**, *113*, 1210–1217.
- (46) Tan, X. *Diatomix*; CyberWit: Santa Clara, CA, 2004.
- (47) Maksyutenko, P.; Parker, D. S. N.; Zhang, F.; Kaiser, R. I. An LIF Characterization of Supersonic BO and CN Radical Sources for Crossed Beam Studies. *Rev. Sci. Instrum.* **2011**, *82*, 083107/083101–083107/083107.
- (48) Gu, X. B.; Guo, Y.; Kawamura, E.; Kaiser, R. I. Design of a Convection-Cooled, Cluster-Based Voltage Divider Chain for Photomultiplier Tubes. *Rev. Sci. Instrum.* **2005**, *76*, 083115/083111–083115/083116.
- (49) Guo, Y.; Gu, X.; Kawamura, E.; Kaiser, R. I. Design of a Modular and Versatile Interlock System for Ultrahigh Vacuum Machines: A Crossed Molecular Beam Setup as a Case Study. *Rev. Sci. Instrum.* **2006**, *77*, 034701/034701–034701/034709.
- (50) Vernon, M. Thesis, University of California, Berkeley, 1981.
- (51) Weis, M. S. Ph.D. Thesis, University of California, Berkeley, 1986.
- (52) Becke, A. D. Density-Functional Thermochemistry. III. The Role of Exact Exchange. *J. Chem. Phys.* **1993**, *98*, 5648–5652.
- (53) Lee, C.; Yang, W.; Parr, R. G. Development of the Colle-Salvetti Correlation-Energy Formula into a Functional of the Electron Density. *Phys. Rev. B* **1988**, *37*, 785–789.
- (54) Pople, J. A.; Head-Gordon, M.; Raghavachari, K. Quadratic Configuration Interaction. A General Technique for Determining Electron Correlation Energies. *J. Chem. Phys.* **1987**, *87*, 5968–5975.
- (55) Purvis, G. D.; Bartlett, R. J. A Full Coupled-Cluster Singles and Doubles Model: The Inclusion of Disconnected Triples. *J. Chem. Phys.* **1982**, *76*, 1910–1918.
- (56) Scuseria, G. E.; Janssen, C. L.; Schaefer, H. F., III. An Efficient Reformulation of the Closed-Shell Coupled Cluster Single and Double Excitation (CCSD) Equations. *J. Chem. Phys.* **1988**, *89*, 7382–7387.
- (57) Scuseria, G. E.; Schaefer, H. F., III. Is Coupled Cluster Singles and Doubles (CCSD) More Computationally Intensive Than Quadratic Configuration Interaction (QCISD)? *J. Chem. Phys.* **1989**, *90*, 3700–3703.
- (58) Dunning, T. H., Jr. Gaussian Basis Sets for Use in Correlated Molecular Calculations. I. The Atoms Boron through Neon and Hydrogen. *J. Chem. Phys.* **1989**, *90*, 1007–1024.
- (59) Peterson, K. A.; Dunning, T. H., Jr. Intrinsic Errors in Several ab Initio Methods: The Dissociation Energy of N₂. *J. Phys. Chem.* **1995**, *99*, 3898–3901.
- (60) Frisch, M. J.; Trucks, G. W.; Schlegel, H. B.; Scuseria, G. E.; Robb, M. A.; Cheeseman, J. R.; Zakrzewski, V. G.; Montgomery, J. A.; Stratmann, R. E.; Burant, J. C.; et al. *Gaussian 98*, revision A.11; Gaussian, Inc.: Pittsburgh, PA, 2001.
- (61) Werner, H.-J.; Knowles, P. J.; Amos, R. D.; Bernhardsson, A.; Berning, A.; Celani, P.; Cooper, D. L.; Deegan, M. J. O.; Dobbyn, A. J.

Eckert, F.; Hampel, C.; Hetzer, G.; et al. MOLPRO, a package of ab initio programs, version 2002.1.

(62) Stanton, J. F.; Gauss, J.; Watts, J. D.; Szalay, P. G.; Bartlett, R. J.; et al. *ACES II-MAB*, the Mainz-Austin-Budapest version (see <http://www.aces2.de>).

(63) Eyring, H.; Lin, S. H.; Lin, S. M. *Basic Chemical Kinetics*; Wiley: New York, 1980.

(64) Robinson, P. J.; Holbrook, K. A. *Unimolecular Reactions*; Wiley: New York, 1972.

(65) Steinfield, J. I.; Francisco, J. S.; Hase, W. L. *Chemical Kinetics and Dynamics*; Prentice Hall: Engelwood Cliffs, NJ, 1999.

(66) Zhang, F.; Gu, X.; Kaiser, R. I.; Bettinger, H. A. Reinvestigation of the Gas Phase Reaction of Boron Atoms, $^{11}\text{B}(^2\text{P}_j)/^{10}\text{B}(^2\text{P}_j)$ with Acetylene, $\text{C}_2\text{H}_2(X^1\Sigma_g^+)$. *Chem. Phys. Lett.* **2008**, 450, 178.

(67) Levine, R. D. *Molecular Reaction Dynamics*; University of Cambridge: Cambridge, UK, 2005.

(68) Wenthold, P. G.; Kim, J. B.; Jonas, K.-L.; Lineberger, W. C. An Experimental and Computational Study of the Electron Affinity of Boron Oxide. *J. Phys. Chem. A* **1997**, 101, 4472.